Journal of Materials Chemistry A

Accepted Manuscript

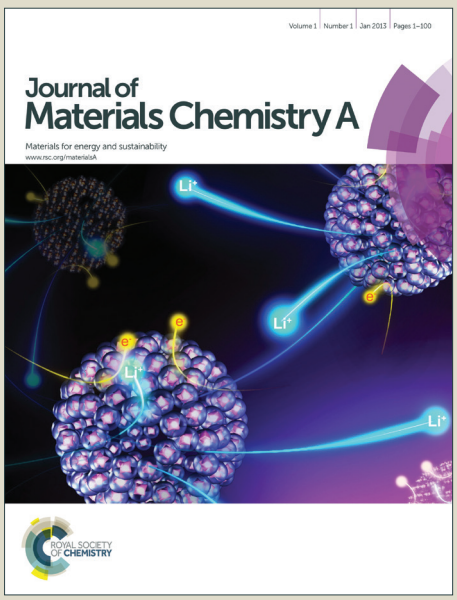

ROYAL SOCIETY OF CHEMISTRY

www.rsc.org/materialsA

Journal Name

RSCPublishing

ARTICLE

Carbides of group IVA, VA and VIA transition metals as alternative HER and ORR catalysts and support materials

Cite this: DOI: 10.1039/xoxxooooox

Received ooth January 2012,
Accepted ooth January 2012

DOI: 10.1039/xoxxooooox

www.rsc.org/

Yagya N Regmi, Gregory R Waetzig, Kyle D Duffee, Samantha M Schmuecker, James M Thode and Brian M Leonard*

High surface area nano dimensional carbides of nine transition metals in group IV-VI have been synthesized using a salt flux method. Uniformity was maintained throughout the investigation, from synthesis method to electrochemical tests, so that comparison can be made for the various carbides for their catalytic activities towards hydrogen evolution reaction (HER) and oxygen reduction reaction (ORR). Catalytic activities are dependent on synthesis method which determines the properties of the catalyst, and electrochemical conditions. Maintaining uniformity throughout the investigation allows for a more balanced comparison of a family of materials. Activity of all nine carbides show increased HER activity compared to bare glassy carbon working electrode. Mo_2C, WC and V_8C_7 show particularly enhanced HER activity. Similarly, Mo_2C, Cr_3C_2 and V_8C_7 have significant ORR activities. Using a wet impregnation method, dispersed platinum nanoparticles ranging between 3 and 5 nm were successfully deposited on the carbides. The Pt deposited carbides have as much as three times higher HER activity and four times ORR activity compared to commercially available Pt/C catalyst, and show enhanced stability under fuel cell conditions.

Introduction

To alleviate mankind's reliance on fossil fuels for future energy needs, fuel cells are seen as an attractive alternative source of energy due to their clean byproduct (water) compared to the harmful oxides of carbon, sulfur and nitrogen that fossil fuels produce.[1] Development of more efficient fuel cells has been hampered by the lack of abundant, cost effective, and durable alternatives to the standard catalyst, platinum on carbon.[2] In addition, a greener source of the fuel used in proton exchange membrane fuel cells (PEMFC), hydrogen, is also desirable because the majority of hydrogen is currently produced by steam reforming hydrocarbons.[3]

One promising route to greener water splitting methods is the hydrogen evolution reaction (HER). This will facilitate the move away hydrocarbons as the source of hydrogen, however HER needs to be optimized as well. Identification of affordable, abundant and yet superior HER and oxygen reduction reaction (ORR) catalysts are critical for PEMFCs to make fuel cell technology more viable alternative sources of energy.

Transition metal carbides (TMC) have received considerable attention as alternative electrocatalysts and supporting materials due to either a decrease in the amount of platinum required or in some cases complete removal of the precious metal.[4,5] Specifically, carbides of Group 4-6 TMs have been investigated extensively for their catalytic properties towards various reactions including HER,[6] ORR[7] and oxygen evolution reaction (OER).[8] These TMs form stable carbides, including multiple stoichiometries and polymorphs, that are resistant to electrochemical corrosion.[9] Well established synthesis methods, such as salt flux synthesis and temperature programmed reduction (TPR), have been developed to increase

Department of Chemistry, University of Wyoming, 1000 E University Avenue, Laramie, 8207, USA.
Email: bleonar5@uwyo.edu

Electronic Supplementary Information (ESI) available: Experimental details, XRD, BET, ICP-MS, TEM and electrochemical data. See DOI: 10.1039/b000000x/

the range of carbide materials available and to lower the cost of synthesizing these carbides.[10, 11]

Salt flux systems above their melting temperatures facilitate enhanced diffusion of precursors thus lowering the temperature and time while improving reproducibility of the synthesis method.[12] Eutectic mixtures of halide salts have been used to synthesize carbides at relatively low annealing temperatures because the halide salt eutectics have low melting points and are inert to final TMC products.[10] Additionally, the use of salt flux as synthesis matrix thus minimizes the costs associated with high annealing temperatures (>1400°C) and long annealing times required in traditional heat and beat method. Using MWCNT as a template, in addition to source of carbon, improves control over the purity and morphology, which traditional carbide synthesis methods lack.[13]

Molybdenum and tungsten carbides of various stoichiometries, crystal structures and morphologies have been studied as HER and ORR catalysts.[14] Recently, it has been shown that several phases of molybdenum carbide are active HER catalysts; reiterating the possibility that a library of TMC materials would result in better optimization of catalytic materials.[15] Other TMCs of this region of the periodic table have received very sporadic attention, as electrochemical catalysts. TiC has been investigated predominantly as a stable support material for ORR, owing to its low activity but stability in acidic and basic mediums.[16] Other TMCs such as ZrC, Nb_4C_3 and HfC also show negligible activity compared to molybdenum carbide, but they have been shown to be very hard, durable and corrosion resistant materials.[17] Thus, they also can be used as support materials in conditions such as extreme pH and highly reducing/oxidizing environments where molybdenum and tungsten carbides have been reported to suffer from short and long term instability.[18,19] Vanadium and chromium carbides have been explored as catalysts as well as support materials for ORR and HER respectively. Platinum supported on V_8C_7 showed much higher ORR mass activity compared to Pt/C[20] and HER overpotential was shown to be dependent on the stoichiometry of the chromium carbide.[21] Partially oxidized TaC has also shown appreciable electrochemical activities towards ORR.[22]

Although the efforts to identify better catalysts have seen a surge recently, there is a distinct lack of uniformity across the methods adopted to synthesize and to measure the catalytic activities. Thus, the comparison of the reported measurements of the carbides and other catalysts is difficult. While some variables such as choice of reference electrodes and catalyst loading can be either mathematically interconverted or normalized, others, such as electrolytes, cannot. For a fair comparison of the catalytic activities of a family of materials, like early TM carbides, uniformity starting with synthesis method to electrochemical measurement conditions is desirable. With this in mind, we have synthesized TMCs of the nine elements belonging to the first three periods of groups 4-6 using a salt flux method. The same synthesis procedure as well as characterization and catalytic activity measurement methods were used for all nine TMCs. The TMCs were tested for HER and ORR activities under identical electrochemical conditions. Additionally, platinum was deposited on the TMCs using a wet impregnation method to compare them as HER and ORR catalyst supports. Comparisons of HER and ORR mass activities (per milligram of platinum) of platinum deposited TMCs along with the standard Pt/C are presented.

Experimental

Materials

The following metal powders and salts were purchased from Aldrich and used as received: Ti (100 mesh), V (325 mesh), Cr (100 mesh), Zr (100 mesh, in 1:10 pentanol: water as stabilizer), Mo (99.9% < 150 µm), Hf (325 mesh), Ta (325 mesh), W (12 µm), LiCl, KCl, NaCl and KF. Multiwalled carbon nanotubes (MWCNT, 6-9 nm × 5 µm and 95% C), Pt on graphitized carbon (10 wt % Pt), chloroplatinic acid hydrate (99.9%), Nafion (5 wt % containing 15-20 % water in a solution of low carbon aliphatic alcohols), HNO_3 (70%) and $HClO_4$ (70%) were also purchased from Aldrich. Nb (325 mesh) was purchased from Alfa Aesar and NaF from Mallinckrodt. Pt ICP standard (1000 ppm in 5 wt% HCl) was obtained from Fluka. HCl (12.1 Normal) was obtained from Fisher Scientific.

Synthesis of TMCs

A salt flux method was utilized to synthesize the TMCs. The composition of the salt flux, annealing temperatures and times are listed in table S1 in electronic supplementary information (ESI). MWCNTs, elemental metals, and the salts used are all anhydrous and stored in an Ar filled glovebox. The synthesis of TiC is used as an example of a typical synthesis of TMC. The salt mixture (LiCl:KCl:KF = 58:40:2) was mixed with equimolar quantities (2×10^{-3} moles) of Ti (0.0957 g) and C (0.0240 g) and ground thoroughly using a mortar and pestle inside an Ar glovebox. Then the resulting mixture was transferred to an alumina crucible boat and placed in a furnace under a flow of Ar gas. The furnace was ramped to the annealing temperatures at 100 °C/min and annealed for the specific times listed in table S1 (ESI). The powders were allowed to cool to room temperature and then washed 3 times with deionized (DI) water via sonication and centrifuged to ensure all the salts were washed away from the product. The final precipitate was dried overnight at 50°C and then ground to a fine powder for characterization, electrochemical tests and further modifications.

Synthesis of Pt/TMC

Chloroplatinic acid and TMC were weighed to achieve 10% platinum loading by weight and mixed in a mortar and pestle. 2.0 mL of acetone was added to the mixture to dissolve chloroplatinic acid and the mixture was ground until all the acetone evaporated. The mixture was then transferred to an alumina boat and annealed at 300°C for 6 hours under H_2 (5%

in Ar) flow. The resulting sample was ground to a fine powder for characterization and electrochemical tests.

Characterization of TMCS and Pt/TMCs

X-Ray diffraction (XRD) measurements were performed on a Bruker-AXS Smart Apex II CCD diffractometer equipped with an Oxford Cobra Cryosystem utilizing Mo as the X-Ray source. Brunauer–Emmett–Teller (BET) method was performed to determine specific surface area on a Micromeritics ASAP2020 instrument using N_2 adsorption data at relative pressure from 0.05 to 0.25. Scanning electron microscopy (SEM) studies were carried out on FEI Quanta FEG 450 field emission scanning electron microscope. The SEM was equipped with a secondary electron detector, a backscattered electron detector and an Oxford Inca energy dispersive x-ray detector (EDS). All SEM samples were deposited on a carbon tape for analysis and the acceleration voltage was 20kV. A FEI Tecnai G2 F20 200 kV (S) Transmission Electron Microscope (TEM) was used to characterize the morphology of the TMCs and size of the Pt nanoparticles loaded via wet impregnation method. The TEM samples were prepared by sonicating 10 mg of sample in 5 ml of ethanol for 20 min and drop casting 100 µL of the resulting suspension on Formvar Film 400 square mesh copper grids. Samples for Inductively Coupled Plasma Optical Emission Spectrometry (ICP-OES) were prepared by dissolving 2 mg of the Pt/TMC samples in 2 mL aqua regia (HNO_3:HCl = 1:3) followed by serial dilution using 18.2 MΩ water to obtain 10 ppm Pt concentration. ICP-OES analysis was performed on Perkin Elmer Optima 8300 instrument equipped with Perkin Elmer S10 auto sampler and WinLab 32 software for analysis to determine the Pt-loading in Pt/TMC.

Electrochemical Tests

All electrochemical tests were carried out using the EC potentiostat and a three electrode rotating disk electrode (RDE-2) from BASi with modified 3 mm diameter glassy carbon electrode (GCE) as the working electrode, Ag/AgCl (3 M NaCl) as reference and platinum wire as the counter electrodes. All potentials were adjusted to reversible hydrogen electrode (RHE) based on equation S1 (ESI). The GCE was cleaned by polishing, followed by sonication for 10 minutes and finally by running 10 CV cycles from 800 to -600 mV at 50 mV/s. The GCE was modified by depositing 3 µL of ink resulting in a catalyst loading of 0.28 mg/cm^2 catalyst. The ink suspension was prepared by sonicating 2.5 mg catalyst in 312.5 µL (18.2 MΩ ultrapure) water and 62.5 µL Nafion for 30 minutes. The electrode was then dried at 50°C for at least two hours prior to electrochemical tests. All electrochemical tests were performed in 30 mL of a 0.1M $HClO_4$ (pH = 1) solution. For HER, the electrolyte was degassed for 20 minutes with argon gas. For pure TMCs, the linear sweep voltammetry (LSV) was scanned from -44 to -344 mV at 2 mV/s. For Pt/TMCs the LSV was scanned from 56 to -144 mV at 2 mV/s. ORR studies were carried out by saturating 30 mL electrolyte with pure O_2 for 20 minutes and then scanning the LSV from 856 to 56 mV for TMCs and 1056 to 256 mV for Pt/TMCs at 50 mV/s. Constant potential electrolysis (CPE) stability tests were carried out by taking measurements at 5 s time intervals for 12 hours at -69 mV for Pt/TMC and -294 mV for TMC systems.

Results and Discussion

Synthesis of TMCs and Pt/TMCs

Phase pure carbides were synthesized for most TMC systems by annealing a mixture of metal and MWCNTs for 12 hours at 950°C in the eutectic salt flux composed of 58:40:2 ratio of LiCl:KCl:KF. Compositions of the eutectic salt flux, annealing temperature, and times for the nine TMCs investigated are listed in table S1 (ESI). WC requires slightly higher annealing temperature (1050°C), longer time (36 hrs) and a different flux composed of 41:59 of NaF to NaCl. TiC can be synthesized at a much shorter annealing time (5 hrs). HfC is formed at much lower annealing temperature (750°C) compared to rest of the TMCs studied here. XRD patterns of the final products in figure 1 reveal that the products are crystalline powders with very little to no impurities. Previous attempts to synthesize phase pure WC using various salt flux methods have persistently produced secondary phases such as W_2C and metallic W.[23] Numerous other methods to synthesize WC have been reported ranging from highly engineered complex methods to one step direct pyrolysis of precursors. [24,25] Salt flux synthesis method employed here also contains minute but persistent impurities in the form of elemental tungsten, indicated by * in figure 1. Post synthesis modifications such as acid treatment can be employed to improve the WC phase purity, but were not done to maintain uniformity throughout the nine TMC. Similarly, HfC contains small amount of oxide impurities indicated by the broad peak around 12 two-theta degrees in figure 1.

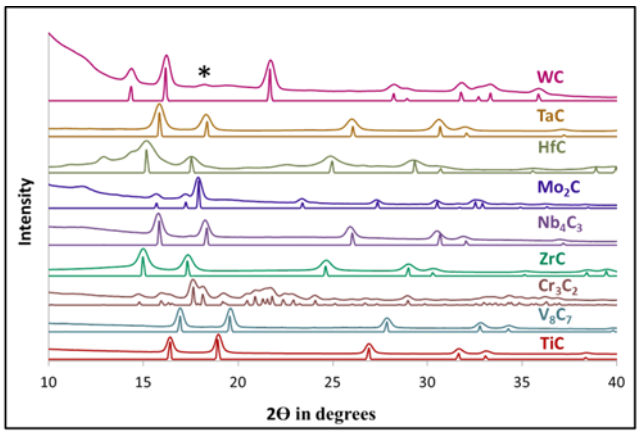

Figure 1: XRD patterns of TMCs synthesized via salt flux method. The reference PDF numbers are WC (00-025-1047), TaC (00-035-0801), HfC (03-065-8749), Mo_2C (00-011-0680), Nb_4C_3 (01-070-8416), ZrC (00-035-0784), Cr_3C_2 (01-074-7137), V_8C_7 (01-089-2608), TiC (01-089-3828)

Most TMCs template onto the MWCNT structure and form either carbide nanotubes or a network of tubular structures as apparent from figure 2. However, TiC, V_8C_7, and Nb_4C_3 do not

template on MWCNT, instead they form flakes of various shapes as can be seen in figure 2a, 2b and 2e respectively. ZrC (2d), HfC (2g) and TaC (2h) adopt the nanotube morphology while Cr_3C_2 (2c), Mo_2C (2f) and WC (2i) form a network of tubular structures with the diameter of the tubes noticeably bigger than the precursor MWCNTs. BET surface areas listed in table S2 (ESI) vary from 7.16 m^2/g for V_8C_7 to 40.73 m^2/g for HfC. The BET surface areas are significantly higher than the carbides prepared from traditional arc-melting method and comparable to other advanced methods such as temperature programmed reaction (TPR) method.[26]

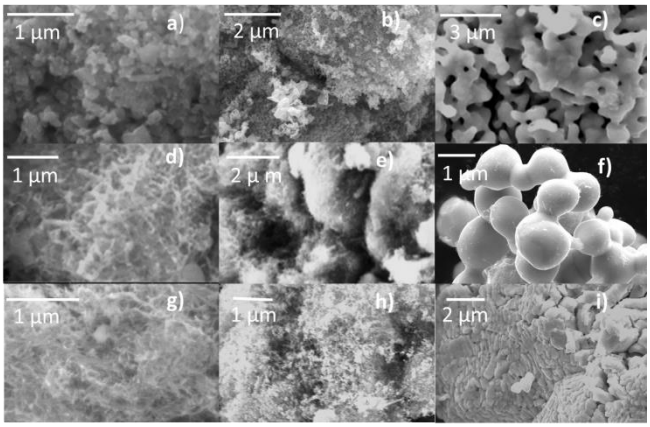

Figure 2: SEM micrographs of a) TiC b) V_8C_7 c) Cr_3C_2 d) ZrC e) Nb_4C_3 f) Mo_2C g) HfC h) TaC i) WC

10% platinum by weight was deposited on the as made TMCs using the wet impregnation method as indicated by XRD pattern in figure S1 (ESI) and the composition was confirmed by ICP-OES seen in table S3 (ESI). The actual weight percentage of platinum deposition was roughly 10% for all TMCs except Mo_2C and WC.

The deposited Pt formed dispersed nanoparticles between 3 to 5 nm on the TMCs as seen in figure 3. Irrespective of the TMC surface area or morphology, both the particle sizes and distribution of the deposited Pt nanoparticles appear uniform. The TEM micrographs in figure 3a and 3c show that the darker Pt nanoparticles are distributed evenly along the TMC nanotubes of Mo_2C and WC. SEM images in figure 2 fail to reveal a tubular morphology and the size of the templated nanotubes of Mo_2C and WC, but TEM micrographs in figure 3 reveal that WC and Mo_2C also template well on MWCNTs. Figures 3b and 3d show that the deposited Pt nanoparticles are about 5 nm in width and the carbide nanotubes are highly crystalline. Similarly, figure 3e and 3f reveal distribution of Pt nanoparticles, about 5 nm in width, on non-tubular TiC and crystalline nature of TiC itself. SAED micrographs shown in insets of figure 3a, 3c and 3e reveal an additional diffraction ring corresponding to Pt (002) between the two diffraction rings corresponding to the TMCs. This is further evidence that Pt is indeed deposited on crystalline TMCs. The d-spacing determined from line profile in figure S2 (ESI) for Pt/WC reveal that the WC (010) surface has slightly higher d-spacing in figure S2b than Pt (002) in figure S2c. Theoretical d-spacing listed in table S4 (ESI), for WC (010) and Pt (111) are 0.252 nm and 0.196 nm respectively while the measured average d-spacing from figure S2b and S2c are 0.258 nm and 0.208 nm.

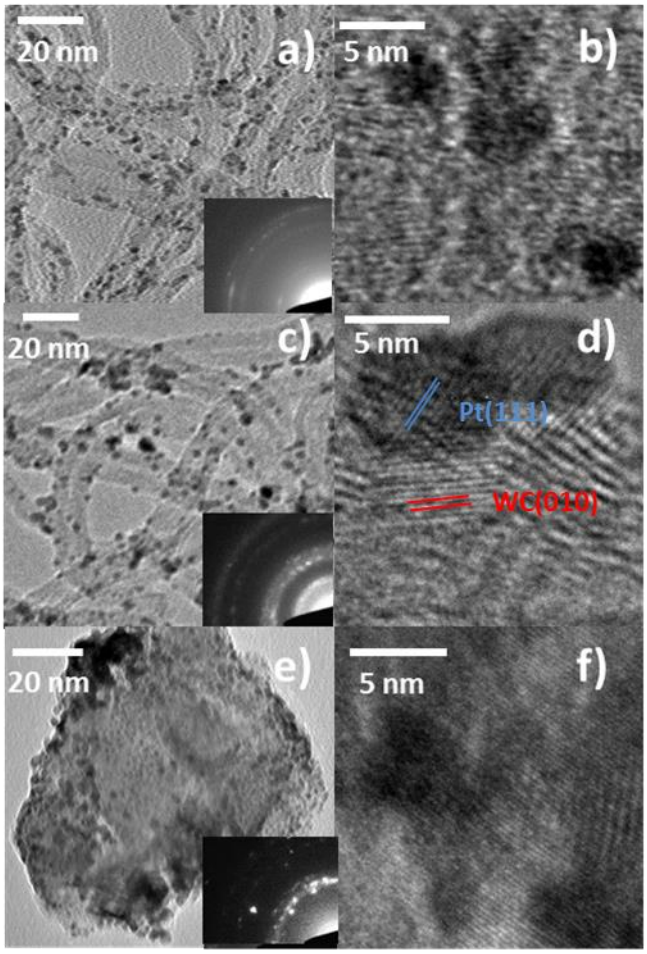

Figure 3: TEM micrographs of Pt/Mo_2C (a and b), Pt/WC (c and d) and Pt/TiC (e and f). Insets in a, c and e are diffraction patterns for Mo_2C, WC and TiC respectively.

TMCs as HER catalysts

TMCs were deposited on a glassy carbon working electrode and tested for HER in 0.1M $HClO_4$ with Ag/AgCl as the reference and Pt wire as counter electrodes respectively. All applied potentials were then adjusted to RHE using equation S1 (ESI). A more positive onset potential and a larger slope of HER curve beyond the onset potential for a system signifies a more efficient catalytic process and thus, a better HER catalyst. Mo_2C has the most positive HER onset potential (around -244 mV) as well as the highest current density (-1.6 mA/cm^2 at -344 mV) as apparent from figure 4. Mo_2C is followed by WC in terms of both onset potential (slightly higher than -244 mV) and current density (0.725 mA/cm^2 at -344 mV)). Although other TMCs show lower HER activities and more negative onset potentials, all of them show significantly enhanced activities and more positive onset potentials compared to the bare glassy carbon working electrode as evident from the inset in figure 4

and bar graph in figure S3 (ESI). V_8C_7 and Cr_3C_2 are of particular interest because they have lower specific surface areas (7.16 and 18.53 m^2/g respectively) compared to Mo_2C and WC (31.32 and 38.54 m^2/g respectively) and yet generate the next highest HER current among the other TMCs. A fairer comparison of their HER activities will require modification in the synthesis method to obtain carbides of V and Cr with specific surface areas closer to 30 m^2/g and then test for electrochemical activities.

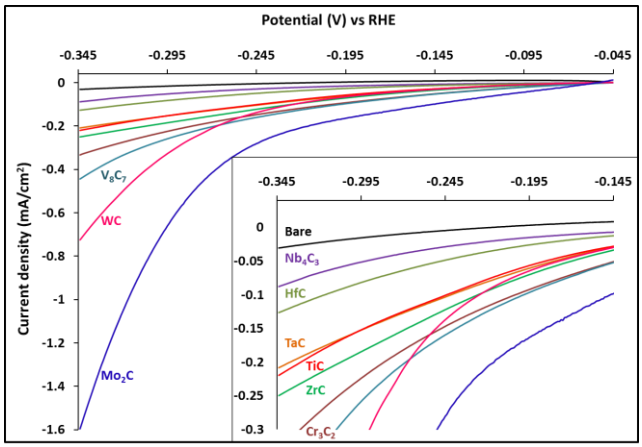

Figure 4: HER current density of TMCs at 2 mV/s and 2500 rpm in 0.1 M $HClO_4$. The inset represents area from 0 to -0.3 mA/cm^2. The curve labelled 'Bare' represents unmodified glassy carbon electrode.

A comparison of the Tafel slopes in figure S4 for HER polarization curves from figure 4 reveals that the HER reaction pathway is slightly different for Mo_2C and WC than rest of the TMCs. From table S5 it can be seen that the Tafel slopes for Mo_2C is 124.8 mV/dec and 137.1 mV/dec for WC which are similar to those reported for Mo_2C and WC synthesized via other methods under similar electrochemical conditions.[15] The Tafel slopes for other TMCs are all greater than 200 mV/dec. Exchange currents derived from Tafel slopes in figure S4 and listed in table S5 for TMCs also follow the same trend as the Tafel slopes. While Tafel slopes and exchange currents on their own cannot be used to predict the exact reaction mechanism for HER, it can be asserted that HER catalyzed by Mo_2C and WC follow different pathways than those of other TMCs.[27]

Long term stability under operational electrochemical conditions is also an important factor to be considered for these TMCs to be viable catalysts. The four most active TMCs were tested for HER stability using controlled potential electrolysis (CPE) at -294 mV for twelve hours. The CPE data seen in the inset in figure S3 (ESI) reiterate that besides the two most active TMCs Mo_2C and WC, V_8C_7 and Cr_3C_2 generate significant amount of HER currents and show remarkable stability. The graph also shows a gradual increase in activity over time for three of the four TMCs tested, Cr_3C_2 being the exception. In comparison, this data demonstrates that with due modifications to optimize activity via increasing the specific area and modifying electronic properties, these carbides may provide cost effective alternative routes for water splitting to generate hydrogen. These nine TMCs provide particularly intriguing prospects because most of these elements form multiple phases of TMCs.[4] If the synthesis methods can be optimized to obtain various phases of these carbides the spectrum of carbide HER catalysts available will be expanded even further.

TMCs as ORR catalysts

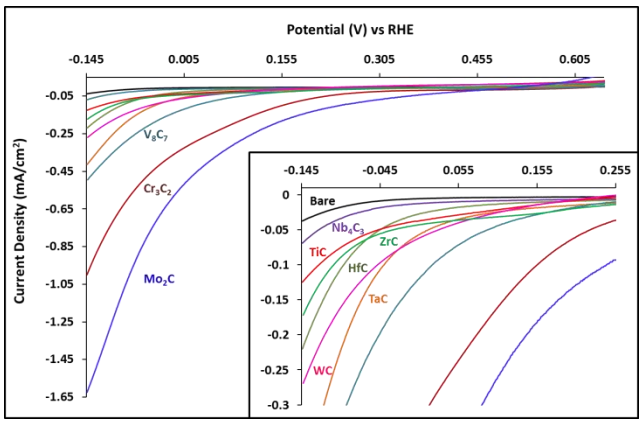

Figure 5: ORR current density of TMCs at 50 mV/s and 1600 rpm in 0.1 M $HClO_4$. The inset represents area from 0 to -0.3 mA/cm^2. Curve labelled 'Bare' represents unmodified glassy carbon electrode.

Analogous to HER, Mo_2C is also the most active ORR catalyst both in terms of onset potential (around 0 mV vs RHE) and current density (-1.6 mA/cm^2 at-144 mV) as seen from figure 5 and figure S5 (ESI). Unlike for HER studies however, Cr_3C_2, V_8C_7 and TaC show higher activity as well as more positive onset potentials than WC. All nine TMCs exhibit markedly improved ORR activities as well as more positive onset potentials in comparison to a bare glassy carbon working electrode as illustrated in the bar graph in figure S5 (ESI). Cr and V systems again provide exciting opportunities for further investigations, such as bifunctional electrocatalysts as both HER and ORR catalysts. Contrary to HER, where it showed significantly reduced activity, TaC demonstrates comparable ORR activity to V_8C_7. When the two most active TMCs, Mo_2C and Cr_3C_2 were tested for stabilities under ORR conditions over a 1000 cycles they showed very little sign of degradation in terms of onset potential and currents as apparent from the inset in figure S5 (ESI).

TMCs as catalyst supports for HER

The HER and ORR activities of the TMCs discussed so far are very promising, and provide opportunities to further improve their activities. They can however have a more immediate impact as improved catalyst support materials. In figure 6, most of the platinum deposited TMC systems show better catalytic activities than commercially available Pt/C which is presently the most widely used fuel cell catalyst.[28] The onset potential of Pt/TMC is roughly about 200 mV more positive than TMC on its own and most of this increase can be attributed to the presence of Pt. Reducing this 200 mV difference on overpotential is a challenge for the medium and

long term. As an incentive to attain short term goals of reducing the cost of fuel cells, figure 6 shows that all the platinum deposited carbides except for ZrC, V_8C_7 and TiC show better activity than Pt/C. Pt/Mo_2C shows the highest HER current density for Pt/TMC systems at -144 mV (about -16 mA/cm^2) which is consistent with the HER activity of Mo_2C for TMC in figure 4. Pt/TaC and Pt/Nb_4C_3 show a relatively enhanced activity even though they have low activities as TMCs. When compared to HER activities for each of the 9 TMCs in figure 4, the corresponding platinum deposited Pt/TMC complexes in figure 6 have approximately a tenfold enhanced activity within about 100 mV of the average onset potential. Thus, the electronic interaction between these carbides and Pt must be facilitating the higher HER activities. Additionally, the variation in activities among the systems, when the activity of the pure TMC is compared to corresponding Pt/TMC, indicate that the Pt-carbide interaction plays a vital role in the electrocatalytic activities. TaC on its own in figure 4 shows inferior HER activity compared to Mo_2C and WC. However, Pt/TaC in figure 6 however shows comparable activity to those of Pt/Mo_2C and Pt/WC.

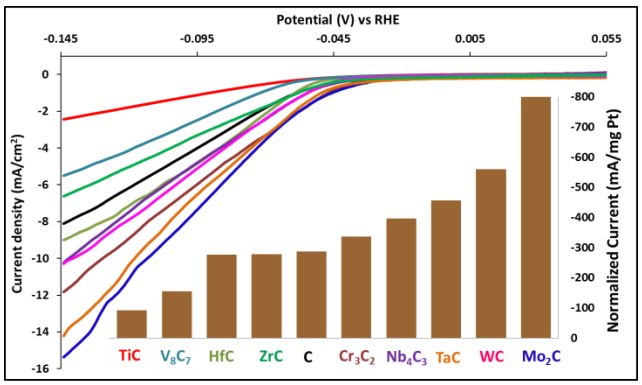

Figure 6: HER current densities for Pt/TMCs measured at 2 mV/s and 2500 rpm in 0.1 M $HClO_4$. The potentials are adjusted to RHE. The bar graph represents the current at –144 mV normalized to mg of Pt. C represents commercial Pt on graphitized carbon.

When the HER activities of Pt/TMC are normalized to mg of Pt loading on the TMCs, based on the ICP-OES data from table S2, the positive impact of TMCs as catalyst support becomes even more apparent. From the bar graph in figure 6, it can be seen that every TMC has enhanced activity compared to Pt/C at -144 mV except for TiC and V_8C_7 after normalization to Pt loading. Pt/Nb_4C_3 shows outstanding normalized activity considering the relatively lower specific surface area Nb_4C_3 possess (table S3 in ESI). So, TMCs as catalyst support materials would make fuel cells more efficient by generating higher activity with the same Pt loading and/or more cost effective by generating same amount of current at lower Pt loading. Pt/Mo_2C generates almost three times the current density (-800 mA/mg Pt) compared to commercial Pt/C (-288 mA/mg Pt) with the same Pt loading.

A comparison of the Tafel slopes in figure S4b and the corresponding exchange currents in table S5 generated from the HER polarization curves in figure 6 shows that most Pt deposited TMCs show similar Tafel slopes but different exchange currents. The synergistic effect of TaC as the Pt support is most apparent when the Tafel slopes and exchange currents are taken into account along with the difference in the HER activity of TaC and Pt/TaC. While TaC has very different Tafel slope and exchange current to Mo_2C and WC, Pt/TaC has comparable values to those of Pt/Mo_2C and Pt/WC in table S5. The Tafel slope and exchange current values are consistent with the values reported from previous investigations under similar electrochemical conditions.[29]

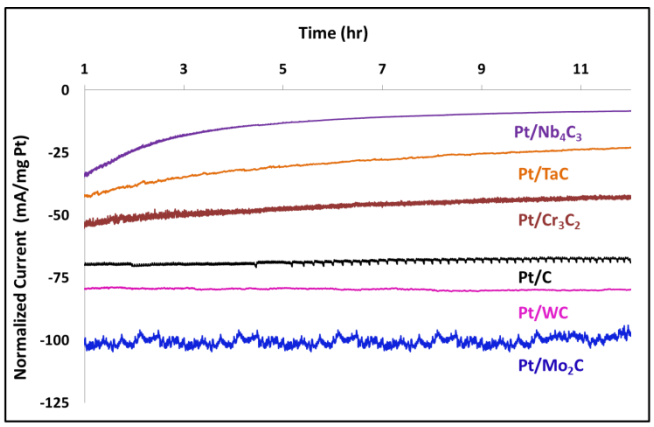

Figure 7: HER current normalized to Pt loading from controlled potential electrolysis for Pt/TMCs measured at -69 mV for 12 hours at 2500 rpm in 0.1 M $HClO_4$.

CPE stability graphs at -69 mV vs RHE in figure 7 reveal that they are stable over twelve hours. From the CPE plots in figure S6 it can be seen that the two most active systems, Pt/Mo_2C and WC, and the corresponding TMC only systems are stable over a 48 hour time period generating the same amount of current densities. The CPE graph for Pt/C shows higher normalized current than Pt/Cr_3C_2, Pt/TaC and Pt/Nb_4C_3 in figure 7 when the bar graph in figure 6 suggests that the Pt/TMC systems should have higher normalized current than Pt/C. A careful look at the graph in figure 6 shows that the current density curves cross each other beyond -69 mV where the CPE measurements were taken. CPE curves recorded at more negative applied potential would correct the anomaly but the increased generation of hydrogen bubbles at higher overpotential creates more noise as can be seen for Pt/Mo_2C. Pt/Cr_3C_2, Pt/TaC and Pt/Nb_4C_3 show initial loss of activity, but show better stability over time. Pt/TMCs show better activity (figure 6) and good electrochemical stability (figure 7) in comparison to current catalyst of choice Pt/C. It is reasonable to speculate that long term stability studies may show that TMCs such as TiC and V_8C_7, which show relatively lower HER activity alone, may be more cost effective in the long term due to their stability compared to Pt/C. TiC particularly shows remarkable stability under harsh electrochemical environments.[8,30] Corresponding CPE curves at higher applied potentials for Pt/TiC system in figure S7 (ESI) show lower

currents, as expected, but stable current densities over 12 hour time periods.

TMCs as catalyst supports for ORR

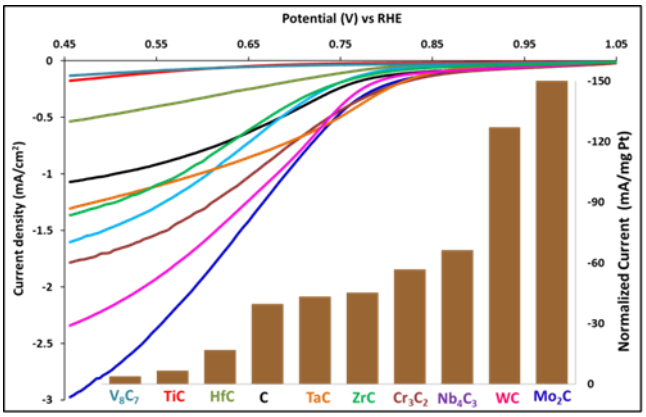

Figure 8: ORR current densities for Pt/TMCs measured at 50 mV/s and 1600 rpm in 0.1 M $HClO_4$. The bar graph represents the normalized current densities at 456 mV vs RHE. C represents commercial Pt on graphitized carbon.

TMCs as ORR catalyst supports show even better activity than as HER catalyst supports when compared to commercial Pt/C. The bar graph in figure 8 indicates that at 456 mV applied potential vs RHE, Pt/Mo_2C system generates almost four times the normalized current (150 mA/mg Pt) and Pt/WC generates more than three times (127 mA/mg Pt) compared to Pt/C (39.5 mA/mg Pt). Nb_4C_3, Cr_3C_2 and ZrC systems also produce significantly higher normalized currents (66, 45 and 57 mA/mg Pt respectively) than Pt/C. Pt/TaC possesses one of the most positive ORR onset potential of all the Pt/TMC systems, but the activity plateaus earlier than other systems as apparent from ORR linear sweep voltammetry graphs in figure 8. Thus, Pt/TaC shows lower activity (43 mA/mg Pt) at 456 mV applied potential compared to the five systems discussed so far, but it still performs better than Pt/C. The sustained increase in activity as the applied potential becomes more negative for most of the Pt/TMC in figure 8 indicates that they can be used in harsher reducing conditions generating higher current than Pt/C, whose activity starts to plateau earlier similar to Pt/TaC system.

Mo_2C shows the highest activities for both HER and ORR, and it is also the best catalyst support for the two electrochemical processes. While a universally acceptable consensus has not been achieved to rationalize the observed superior performance of Mo_2C compared to other TMCs evidence to indicate the favorable electronic interaction of the reactants with molybdenum compounds[31] and highly selective nature of the Mo_2C surfaces are most widely accepted explanations.[32]

Conclusions

From the results we have shown that in addition to Mo_2C and WC all other TMCs of group IV-VI show encouraging HER and ORR activity on their own. Although most of these TMCs have been previously studied for ORR and/or HER, the methods to synthesize the materials and the conditions for electrochemical measurements lacked uniformity. This is the first study where all nine TMCS were synthesized and tested under the same conditions. We have shown that Cr_3C_2 and V_8C_7 show appreciable HER and ORR activities despite the synthesis route employed resulting in relatively lower surface area for these carbides. A modification in synthesis methodology to produce higher surface area Cr_3C_2 and V_8C_7 should result in higher activity for Cr_3C_2 and V_8C_7 in the future. TaC also shows significant ORR activity. The majority of the TMCs also enhance the normalized HER and ORR activities as support materials in Pt/TMC catalyst systems. Mo_2C and WC show significant enhancement in HER and ORR activities as catalyst support in comparison to Pt/C. Pt/Mo_2C shows 4 times ORR and 3 times HER normalized current while Pt/WC produces 3 times the normalized ORR current compared to the commercial system. Nb_4C_3 and Cr_3C_2 are the two most promising systems as ORR and HER catalyst supports besides Mo_2C and WC systems. Pt/Nb_4C_3 and Pt/Cr_3C_2 systems show a remarkable increase in activity when compared to Pt/C despite possessing lower specific surface area carbides. Again, investigations of these two carbides as electrocatalysts supports with modifications in synthesis routes should produce higher specific surface areas and thus improve their HER and ORR activities.

Acknowledgements

This work was supported by The School of Energy Resources at the University of Wyoming. Sincere appreciation goes to Janet Coker Dewey for help with ICP-OES measurements.

References

(1) Debe, M. K. Nature 2012, 486, 43.
(2) Steele, B. C.; Heinzel, A. Nature 2001, 414, 345.
(3) Bolat, P.; Thiel, C. International Journal of Hydrogen Energy 2014, 39, 8898.
(4) Ham, D. J.; Lee, J. S. Energies 2009, 2, 873.
(5) Kimmel, Y. C.; Xu, X.; Yu, W.; Yang, X.; Chen, J. G. ACS Catalysis 2014, 4, 1558.
(6) Wirth, S.; Harnisch, F.; Weinmann, M.; Schröder, U. Applied Catalysis B: Environmental 2012, 126, 225.
(7) He, G.; Yan, Z.; Ma, X.; Meng, H.; Shen, P. K.; Wang, C. Nanoscale 2011, 3, 3578.
(8) Ma, L.; Sui, S.; Zhai, Y. Journal of Power Sources 2008, 177, 470.
(9) Oyama, S. T. Catalysis Today 1992, 15, 179.
(10) Liu, X.; Fechler, N.; Antonietti, M. Chemical Society reviews 2013, 42, 8237.
(11) Claridge, J. B.; York, A. P. E.; Brungs, A. J.; Green, M. L. H. Chemistry of materials 2000, 12, 132.
(12) Bugaris, D. E.; zur Loye, H. C. Angew Chem Int Ed Engl 2012, 51, 3780.

(13) Li, X.; Westwood, A.; Brown, A.; Brydson, R.; Rand, B. Carbon 2009, 47, 201.
(14) Esposito, D. V.; Hunt, S. T.; Kimmel, Y. C.; Chen, J. G. Journal of the American Chemical Society 2012, 134, 3025.
(15) Wan, C.; Regmi, Y. N.; Leonard, B. M. Angew Chem Int Ed Engl 2014, 53, 6407.
(16 Ignaszak, A.; Song, C.; Zhu, W.; Zhang, J.; Bauer, A.; Baker, R.; Neburchilov, V.; Ye, S.; Campbell, S. Electrochimica Acta 2012, 69, 397.
(17)The Chemistry of Transition Metal Carbides and Nitrides; 1 ed.; Oyama, S. T., Ed.; Blackie Academic & Professional: Glasgow, 1996.
(18)Leclercq, G.; Kamal, M.; Lamonier, J. F.; Feigenbaum, L.; Malfoy, P.; Leclercq, L. Appl Catal a-Gen 1995, 121, 169.
(19)Chen, W.-F.; Iyer, S.; Iyer, S.; Sasaki, K.; Wang, C.-H.; Zhu, Y.; Muckerman, J. T.; Fujita, E. Energy & Environmental Science 2013, 6, 1818.
(20)Hu, Z.; Chen, C.; Meng, H.; Wang, R.; Shen, P. K.; Fu, H. Electrochemistry Communications 2011, 13, 763.
(21)Tsirlina, G. A.; Petrii, O. A. Electrochimica Acta 1987, 32, 649.
(22)Ohgi, Y.; Ishihara, A.; Matsuzawa, K.; Mitsushima, S.; Ota, K.-i.; Matsumoto, M.; Imai, H. Electrochimica Acta 2012, 68, 192.
(23)Nersisyan, H. H.; Won, H. I.; Won, C. W. Materials Letters 2005, 59, 3950.
(24)Hunt, S. T.; Nimmanwudipong, T.; Roman-Leshkov, Y. Angew Chem Int Ed Engl 2014, 53, 5131.
(25)Shanmugam, S.; Jacob, D. S.; Gedanken, A. The journal of physical chemistry. B 2005, 109, 19056.
(26)Ramanathan, S.; Oyama, S. T. J Phys Chem-Us 1995, 99, 16365.
(27)Benck, J. D.; Hellstern, T. R.; Kibsgaard, J.; Chakthranont, P.; Jaramillo, T. F. ACS Catalysis 2014, 4, 3957.
(28)Barbir, F. PEM Fuel Cells; 2 ed.; Academic Press: London, 2013.
(29)Liu, Y.; Mustain, W. E. International Journal of Hydrogen Energy 2012, 37, 8929.
(30)Swette, L.; Giner, J. Journal of Power Sources 1988, 22, 399.
(31)Liu, P.; Rodriguez, J. A. Catalysis Letters 2003, 91, 247.
(32)Porosoff, M. D.; Yang, X.; Boscoboinik, J. A.; Chen, J. G. Angew Chem Int Ed Engl 2014, 53, 6705.

For Table of Contents Only:

Nano-carbides were synthesized and tested as catalysts and supports for hydrogen evolution reaction (HER) and oxygen reduction reaction (ORR).